

On the Role of Preference Variance in Preference Optimization

Jiacheng Guo¹, Zihao Li¹, Jiahao Qiu¹, Yue Wu², and Mengdi Wang¹

¹Department of Electrical & Computer Engineering, Princeton University

²AI Lab, Princeton University

ABSTRACT

Direct Preference Optimization (DPO) has emerged as an important approach for learning from human preferences in aligning large language models (LLMs). However, collecting human preference data is costly and inefficient, motivating methods to reduce the required annotations. In this work, we investigate the impact of *preference variance* (PVar), which measures the variance in model preferences when comparing pairs of responses, on the effectiveness of DPO training. We provide a theoretical insight by establishing an upper bound on the DPO gradient norm for any given prompt, showing it is controlled by the PVar of that prompt. This implies that prompts with low PVar can only produce small gradient updates, making them less valuable for learning. We validate this finding by fine-tuning LLMs with preferences generated by a reward model, evaluating on two benchmarks (AlpacaEval 2.0 and Arena-Hard). Experimental results demonstrate that prompts with higher PVar outperform randomly selected prompts or those with lower PVar. We also show that our PVar-based selection method is robust, when using smaller reward models (1B, 3B) for selection. Notably, in a separate experiment using the original human annotations from the UltraFeedback dataset, we found that training on only the top 10% of prompts with the highest PVar yields better evaluation performance than training on the full dataset, highlighting the importance of preference variance in identifying informative examples for efficient LLM alignment.

1 Introduction

The rapid proliferation and increasing sophistication of Large Language Models (LLMs) have marked a transformative phase in artificial intelligence, with these models becoming integral to a wide array of applications and evolving into autonomous agents capable of complex decision-making in real-world scenarios [Ouyang et al., 2022a, Achiam et al., 2023, Kim et al., 2025, Shen et al., 2023, Guo et al., 2025]. LLM alignment refers to the whole process of ensuring that model-generated outputs and behaviors are consistent with these human-centric principles [Ji et al., 2025]. Ensuring LLMs in accordance with human values and expectations has emerged as a critical imperative in society [Christiano et al., 2017, Ziegler et al., 2019, Lee et al., 2021, Huang et al., 2024, 2025].

Reinforcement Learning from Human Feedback (RLHF) is a prevalent approach that fine-tunes an LM policy to maximize a learned reward model derived from human preference comparisons [Christiano et al., 2017, Ouyang et al., 2022a]. This pipeline typically involves a complex multi-stage training process – first fitting a reward model on human preference data, and then performing policy optimization (often via Proximal Policy Optimization, PPO [Schulman et al., 2017]) with careful regularization (e.g. KL penalties) to avoid the model drifting too far from its pre-trained behavior [Ouyang et al., 2022a]. While RLHF has produced impressive results in aligning LLMs with human intent, the complexity and instability of this procedure (training multiple models and sampling in-loop) have motivated research into simpler yet effective methods for preference alignment.

Direct Preference Optimization (DPO) [Rafailov et al., 2023] is an appealing RL-free alternative for preference alignment. Instead of applying a two-stage reward learning and policy optimization procedure, DPO directly fine-tunes a language model on preference pair data using a simple binary classification loss on preference pairs. Specifically, DPO leveraging a pairwise Bradley–Terry preference model [Bradley and Terry, 1952] under the hood, and increases the relative log-probability of preferred responses over dispreferred ones for each prompt without reinforcement learning. Empirically, DPO and its variants [Wu et al., 2024, Azar et al., 2024, Ethayarajh et al., 2024, Zhao et al., 2024, Meng et al., 2024] has been shown to achieve alignment performance comparable to PPO-based RLHF while being more

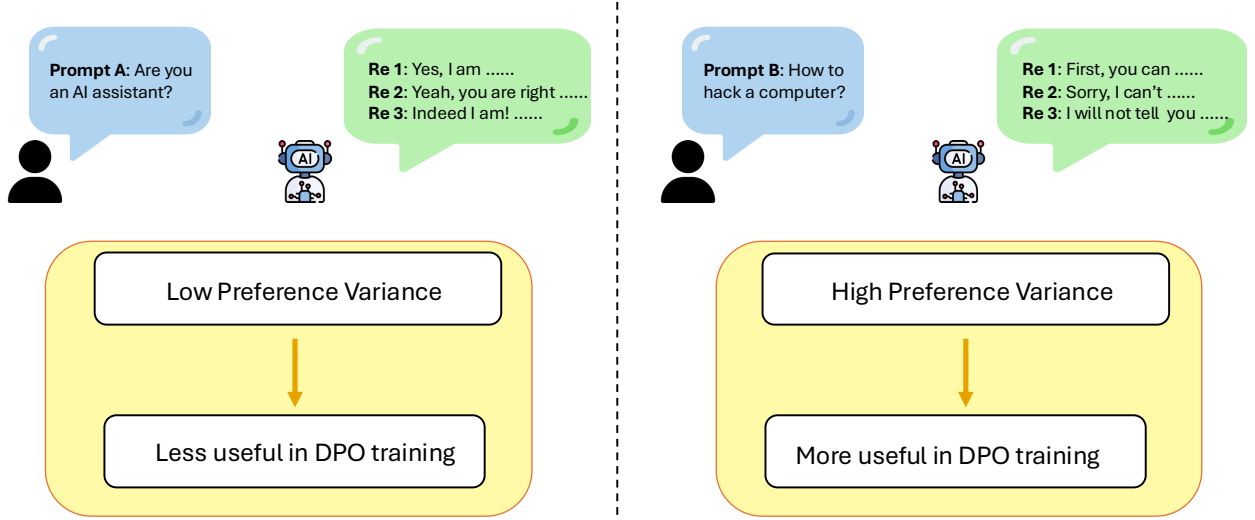


Figure 1: Comparison of prompts with different Preference Variance (PVar). Left: A prompt with low PVar (e.g., 'Are you an AI assistant?'). Responses to such prompts are often semantically similar (e.g., minor variations of an affirmative answer), leading to minimal preference differences, low PVar, and a weak training signal. Right: A prompt with high PVar (e.g., 'How to hack a computer?'). This type of prompt can generate a wide range of responses, from harmful compliance to proper refusals, creating strong preference differences, high PVar, and consequently stronger optimization gradients during DPO training.

stable and straightforward to train, and is cheaper in computation and memory. Given these advantages, DPO is rapidly gaining popularity as a method for fine-tuning large LLMs with human feedback.

A significant practical challenge in implementing DPO (and preference-based alignment in general) is that preference data annotation typically requires human judgment, making it resource-intensive and costly [Deng et al., 2025, Belakaria et al., 2025]. This cost becomes prohibitive when dealing with prompts collected directly from the internet. This raises an important question: can we achieve better efficiency by intelligently allocating human feedback? Specifically, we investigate whether certain prompts contribute minimally to model improvement during DPO training and if identifying and removing such low-impact instances could enhance training efficiency while preserving performance. This motivates our research question:

Can we identify a quantifiable characteristic of prompts that determines their utility for DPO, thereby enabling more efficient data selection for model alignment?

Drawing inspiration from recent studies on the dynamics of RLHF training and reward variance patterns [Feng et al., 2024, Razin et al., 2025], which demonstrate that low reward variance can lead to vanishing gradients in RLHF objectives, we formulate a hypothesis: **prompts generating "similar" responses create weak preference signals, potentially leading to inefficient DPO training.**

To quantify this hypothesis, we introduce Preference Variance (PVar), a metric that quantifies the variability in a model's preference probabilities (i.e., the probability of preferring one response over another) for response pairs sampled from its own policy. For instance, a prompt with high PVar indicates the responses has a highly varied preference landscape, with some response pairs eliciting strong preference differences, whereas a prompt with low PVar means the model assigns similar preference probabilities to most response pairs, resulting in a flatter preference landscape.

Through theoretical analysis, we establish that when PVar approaches zero, the DPO policy gradient magnitude is necessarily small. This finding parallels the observations in RLHF literature that connect low reward variance to optimization difficulties [Feng et al., 2024, Razin et al., 2025]. Figure 1 illustrates this concept with contrasting examples. The left panel shows a prompt with low PVar where an AI assistant responds to a simple identity question, resulting in similarly preferred responses and consequently less useful training signal for DPO. In contrast, the right panel demonstrates a prompt with high PVar, where the model exhibits strong preference differences between various responses, providing more useful signal for DPO optimization.

We then validate our theoretical insights through extensive experiments: we train DPO models on four datasets (UltraFeedback [Cui et al., 2023], Chatbot Arena Conversation [Zheng et al., 2023], HH-RLHF [Bai et al., 2022], and WebGPT [Nakano et al., 2021]), and evaluate the resulting models on two alignment benchmarks (AlpacaEval 2.0

[Dubois et al., 2024] and Arena Hard [Li et al., 2024a,b]). The empirical results confirm our hypothesis – prompts with higher PVar tend to drive larger updates and have outsized impact on alignment performance.

Our main contributions are:

- We provide a theoretical justification for offline data selection by showing that a prompt’s online DPO gradient norm is bounded by its Preference Variance (PVar). We then formally connect this online quantity to a practical, offline PVar estimate, providing a rigorous basis for our selection method.
- We empirically validate this theory by demonstrating that models trained on high-PVar data subsets consistently achieve better performance across multiple models, datasets, and benchmarks. Furthermore, we show that our PVar-based selection is robust, outperforming a common reward gap baseline even when the latter is guided by reward models of varying sizes (1B, 3B, 8B).
- We illustrate the practical implications by using Ultrafeedback with human annotations. We found that selecting only the top 10% highest-PVar prompts for DPO training achieved better performance than using the entire dataset, suggesting that strategically selecting high-PVar prompts can achieve superior alignment with substantially reduced annotation effort.

2 Related Work

In this section, we discuss the related work of our approach. Please refer to Appendix A for additional related work.

DPO and Its Variants. DPO has emerged as a significant advancement in LLM alignment, offering a simpler and more stable alternative to traditional RLHF by eliminating the separate reward modeling stage [Rafailov et al., 2023]. Following its introduction, DPO has gained substantial attention in the alignment community due to its robust performance and implementation simplicity, sparking numerous variant methods [Wu et al., 2024, Azar et al., 2024, Ethayarajh et al., 2024, Zhao et al., 2024, Meng et al., 2024]. These variants address different aspects of the preference learning problem, including extensions to handle ranking beyond pairwise preferences [Chen et al., 2024, Dong et al., 2023, Liu et al., 2024a, Song et al., 2024], simplified objectives that operate without reference models [Hong et al., 2024, Meng et al., 2024]. The broader landscape of preference learning algorithms includes other approaches beyond DPO, such as rejection sampling techniques [Dong et al., 2023, Gulcehre et al., 2023] and alternative RL-based training methods [Li et al., 2023a, Zhong et al., 2024]. Despite the preference learning algorithms, most methods operate under the assumption that large human-annotated preference datasets are readily available, overlooking the substantial data acquisition costs involved. This highlights the practical importance of our work, which potentially reduces the amount of human annotation required while maintaining or improving alignment quality.

Theoretical Analysis in RLHF. The theoretical foundations of RLHF have attracted growing attention as these methods become more central to LLM alignment [Chakraborty et al., 2024, Ding et al., 2024, Chakraborty et al., 2025, Chen et al., 2025a]. Prior theoretical work has primarily focused on developing algorithms to find optimal policy under various technical assumptions [Das et al., 2024a, Du et al., 2024, Ji et al., 2023, Novoseller et al., 2020, Pacchiano et al., 2021, Wang et al., 2023, Wu and Sun, 2023, Xiong et al., 2023, Xu et al., 2020, Li et al., 2023b] or study the sample complexity of estimating a reward model by using a given dataset [Li et al., 2024c, Sun et al., 2025, Li et al., 2024c]. Most closely related to our research, recent investigations have examined the critical influence of reward variance on RLHF objectives [Razin et al., 2023, 2025]. Specifically, [Razin et al., 2023] demonstrated that gradient vanishing occurs under conditions of low reward variance, while [Razin et al., 2025] established that reward variance constitutes a more significant factor than accuracy for reward models in RLHF applications. Our work builds upon these foundational insights, extending their theoretical contributions to the domain of preference learning.

3 Preliminaries

Notations. Let $x \in \mathcal{X}$ represent a prompt $x = [x_1, x_2, \dots, x_n]$, where \mathcal{X} is the space of all possible prompts and x_i being the i -th token in the prompt. Similarly, $y \in \mathcal{Y}$ denotes a response $y = [y_1, y_2, \dots, y_n]$, where \mathcal{Y} is the space of all possible responses and y_i being the i -th token in the response. The language model’s policy is represented as $\pi_\theta(y|x) = \prod_{i=1}^{|y|} \pi_\theta(y_i|x, y_{<i})$, where $\theta \in \mathbb{R}^p$ denotes the model parameters, capturing the probability of generating response y given prompt x . We also have a reference policy $\pi_{\text{ref}}(y|x)$, which is typically the pre-trained or SFT model.

Preference Probability with Rewards and DPO Objective. DPO was originally proposed in Rafailov et al. [2023], and leverages the Bradley-Terry (BT) model [Bradley and Terry, 1952] to formulate preference probabilities between responses. For a better background understanding, we briefly describe its motivation and derivation from RLHF below. In the BT model, the probability that one response y_i is preferred over another response y_j given prompt x is expressed as:

$$\mathbb{P}(y_i \succ y_j|x) = \sigma(r(x, y_i) - r(x, y_j)). \quad (1)$$

where $\sigma(z) = \frac{1}{1+e^{-z}}$ is the sigmoid function and $r(x, y)$ represents a reward function. InstructGPT [Ouyang et al., 2022b] proposes to learn the reward function by maximizing the log likelihood $\log \mathbb{P}(y_i \succ y_j | x)$ as the first step. With the learned reward function, Ouyang et al. [2022b] further learns to fine-tune the original policy by maximizing the following objective:

$$\max_{\theta} \mathbb{E}_{x \sim \mathcal{C}(X), y \sim \pi_{\theta}(\cdot | x)} [r(x, y)] - \beta \mathbb{E}_{x \sim \mathcal{X}} [D_{KL}(\pi_{\theta}(\cdot | x) \| \pi_{\text{ref}}(\cdot | x))], \quad (2)$$

where $\mathcal{C}(X)$ is the distribution of x , $\beta > 0$ is a regularization hyperparameter and D_{KL} is the Kullback-Leibler divergence. The direct optimizer of equation 2 is $\pi_{\theta}(y|x) \propto \pi_{\text{ref}}(y|x) \cdot \exp(\frac{1}{\beta} r(x, y))$. For any policy π_{θ} , Rafailov et al. [2023] proposed to estimate the corresponding implicit reward by re-arranging this relationship:

$$\hat{r}_{\theta}(x, y) = \beta (\log \pi_{\theta}(y|x) - \log \pi_{\text{ref}}(y|x)).$$

Plugging this implicit reward into the BT model in Eq. equation 1, the preference probability becomes a function of the policy π_{θ} :

$$\mathbb{P}(y_i \succ y_j | x) = \sigma(\hat{r}_{\theta}(x, y_i) - \hat{r}_{\theta}(x, y_j)) = \sigma\left(\beta \left[\log \frac{\pi_{\theta}(y_i|x)}{\pi_{\text{ref}}(y_i|x)} - \log \frac{\pi_{\theta}(y_j|x)}{\pi_{\text{ref}}(y_j|x)}\right]\right).$$

In the following part of this paper, we will use $p_{\theta}(x; y_i, y_j)$ to denote $\mathbb{P}(y_i \succ y_j | x)$ for simplicity of notation. DPO then learns the optimal policy by minimizing the negative log-likelihood of the preference data. For a dataset \mathcal{D} of preference pairs (x, y_w, y_l) , where y_w is the winner over the loser y_l , the DPO loss function is defined as:

$$\mathcal{L}_{\text{DPO}}(\theta) = -\mathbb{E}_{(x, y_w, y_l) \sim \mathcal{D}} [\log p_{\theta}(x; y_w, y_l)] = -\mathbb{E}_{(x, y_w, y_l) \sim \mathcal{D}} [\log \sigma(\hat{r}_{\theta}(x, y_w) - \hat{r}_{\theta}(x, y_l))].$$

Minimizing this loss effectively increases the probability of generating preferred responses over less preferred ones, while simultaneously maintaining proximity to the reference model through an implicit regularization mechanism.

Preference Variance (PVar). To quantify the utility of a prompt for DPO, we introduce Preference Variance (PVar). We focus on the variance of preference probabilities, rather than the variance of rewards, because the DPO loss is a function of reward *differences*, not absolute reward values. A prompt could generate responses with high but very similar rewards (low PVar, but potentially high reward variance), providing a weak learning signal for DPO. We now define a key metric in our work: the variance in preference probabilities for a given prompt. For a fixed prompt x , we are interested in characterizing how consistently the model expresses its preferences across different response pairs. Formally, we consider the random variable P_x representing the model’s preference strength when comparing two responses sampled from its own distribution: $P_x = p_{\theta}(x; y_i, y_j)$ where $y_i, y_j \sim \pi_{\theta}(\cdot | x)$ are independently sampled responses. The Preference Variance (PVar) for prompt x under model θ is defined as:

$$\text{PVar}_{\theta}[x] = \text{Var}_{y_i, y_j \sim \pi_{\theta}(\cdot | x)} [p_{\theta}(x; y_i, y_j)].$$

This metric quantifies the variability in the model’s preference judgments across different pairs of candidate responses. A low PVar indicates that the model has similar preference strengths for most response pairs, suggesting a relatively flat preference landscape (i.e., low PVar). Conversely, a high PVar suggests the model has strong and differentiated preferences among its generated responses, with some pairs exhibiting much stronger preference signals than others. PVar directly measures the variability in these critical reward differences as captured by the sigmoid function, thus offering a more direct link to the DPO objective’s optimization landscape.

Estimating PVar in Practice. In practical implementations, we use the Monte Carlo method [Wasserman, 2013] to estimate the empirical PVar by generating n response samples $\{y_1, y_2, \dots, y_n\}$ from an initial policy $\pi_{\theta_0}(\cdot | x)$ and computing pairwise preference probabilities. Furthermore, while the preference probability $p_{\theta}(x; y_i, y_j)$ is defined using an implicit reward function that changes as the policy updates, directly using these implicit rewards for sample selection is impractical. Instead, we employ a fixed, external reward model $r_{\phi}(x, y)$ as a stable estimator for the preference signals. This approach allows us to compute the estimated preference probability:

$$\hat{p}(x; y_i, y_j) = \sigma(r_{\phi}(x, y_i) - r_{\phi}(x, y_j)).$$

The estimated PVar is then computed as:

$$\widehat{\text{PVar}}[x] = \frac{1}{n(n-1)} \sum_{i \neq j} (\hat{p}(x; y_i, y_j) - \bar{p})^2, \quad (3)$$

where \bar{p} is the mean of all pairwise preference probabilities in the sample. By symmetry, we have $\hat{p}(x; y_i, y_j) + \hat{p}(x; y_j, y_i) = 1$, thus $\bar{p} = \frac{1}{2}$. This estimation allows us to quantify the variability in model preferences for offline data selection. It is important to note that the reliability of this PVar estimation is directly dependent on the quality of the external reward model. However, our experiments in Section 5.2 (Table 2) demonstrate that PVar-based selection remains a robust criterion, consistently outperforming a reward-gap baseline even when guided by smaller, less powerful reward models (e.g., 1B and 3B parameters). Our theoretical analysis in Section 4 will formally bridge the gap between this practical offline estimation and the online training dynamics.

4 Theoretical Analysis of DPO Gradient and PVar

In this section, we analyze how PVar affects DPO training dynamics. We first present a foundational result (Theorem 4.1) showing that the online DPO gradient for a given prompt is upper-bounded by its online PVar. We then introduce a new bridging theorem (Theorem 4.2) that connects this online gradient to the practical, offline PVar estimated with an external reward model, providing a solid theoretical foundation for our data selection strategy.

Gradient of DPO Loss. Let $\hat{r}_\theta(x, y) = \beta(\log \pi_\theta(y|x) - \log \pi_{\text{ref}}(y|x))$ be the implicit reward. The DPO loss gradient for a given prompt x and a single preference pair (y_w, y_l) can be expressed as:

$$\nabla_\theta \mathcal{L}_{\text{DPO}} = -(1 - \sigma(\hat{r}_\theta(x, y_w) - \hat{r}_\theta(x, y_l))) \cdot \beta [\nabla_\theta \log \pi_\theta(y_w|x) - \nabla_\theta \log \pi_\theta(y_l|x)].$$

Taking the expectation over preference pairs from the dataset $\mathcal{D}(x)$ for a fixed prompt x gives the full gradient for that prompt.

Online Gradient Bound via Online PVar. We first establish a formal relationship between the magnitude of the DPO gradient and the PVar, both evaluated with respect to the current policy π_θ . This result, inspired by [Razin et al., 2023], shows that prompts with small PVar cannot produce large gradient updates. To formalize this, let $|y|$ be the maximum response length and let $\gamma(x; \theta)$ be an upper bound on the Jacobian norm of the model’s logit function with respect to its parameters. We define the term $C(x, \theta) := 8\beta|y|\gamma(x; \theta)$, which depends on the model’s properties.

Theorem 4.1 (PVar Bounds the DPO Gradient). *For parameters $\theta \in \mathbb{R}^p$ and a specific input $x \in \mathcal{X}$, the norm of the DPO loss gradient is upper bounded by:*

$$\|\nabla_\theta \mathcal{L}_{\text{DPO}}(\pi_\theta, \pi_{\text{ref}}; x)\| \leq C(x, \theta) \cdot \text{PVar}_\theta[x]^{1/3},$$

where $\text{PVar}_\theta[x]$ is the online preference variance for prompt x computed with the policy π_θ , and $C(x, \theta)$ is a term dependent on the model’s Jacobian norm and response length, defined above.

Proof Sketch for Theorem 4.1. The proof involves decomposing the gradient. We partition response pairs into two sets: those with preference probabilities close to 1/2 and those with more extreme preferences. The contribution from the first set is bounded by a threshold parameter c . The probability mass of the second set is bounded by $\text{PVar}_\theta[x]/c^2$ via Chebyshev’s inequality. Combining these bounds yields an expression of the form $K_1 \cdot c + K_2 \cdot \text{PVar}_\theta[x]/c^2$. Optimizing for c gives the final $\text{PVar}^{1/3}$ dependency. The full proof is in Appendix B.

Bridging Offline Selection and Online Dynamics. Theorem 4.1 links the online gradient to online PVar, but in practice we select data using an offline PVar calculated with a fixed reward model r_ϕ and an initial policy π_{θ_0} . The following theorem bridges this gap by bounding the online gradient norm for a specific prompt x using its practical, offline PVar plus several interpretable error terms.

Theorem 4.2 (Offline-to-Online Gradient Bound). *Let $\widehat{\text{PVar}}_{\phi, \theta_0}[x]$ be the offline PVar for a specific prompt x , estimated using a reward model r_ϕ and an initial policy π_{θ_0} . The online DPO gradient norm for that prompt is bounded as:*

$$\|\nabla_\theta \mathcal{L}_{\text{DPO}}(\pi_\theta, \pi_{\text{ref}}; x)\| \leq C(x, \theta) \cdot \left(\widehat{\text{PVar}}_{\phi, \theta_0}[x] + \Xi(x; \theta, \phi) \right)^{1/3},$$

where $C(x, \theta)$ is the same constant as in Theorem 4.1, and $\Xi(x; \theta, \phi)$ is a prompt-specific error term defined as:

$$\begin{aligned} \Xi(x; \theta, \phi) = & \underbrace{2 \sup_y |\hat{r}_\theta(x, y) - r_\phi(x, y)|}_{\text{Policy-Reward Disagreement}} + \underbrace{2 \sup_y |r_\phi(x, y) - r^*(x, y)|}_{\text{Reward Model Error}} \\ & + \underbrace{6 \text{TV}(\pi_\theta(\cdot|x) \otimes \pi_\theta(\cdot|x), \pi_{\theta_0}(\cdot|x) \otimes \pi_{\theta_0}(\cdot|x))}_{\text{Policy Distribution Shift}}. \end{aligned}$$

The error term Ξ consists of three components for a given x : (1) the disagreement between the policy’s implicit reward and the external reward model, (2) the error of the reward model with respect to a ground-truth reward r^* , and (3) the distribution shift of the policy from its initial state π_{θ_0} to the current state π_θ .

Proof Sketch for Theorem 4.2. The proof leverages a triangle inequality argument. For a prompt x , we first relate its online PVar, $\text{PVar}_\theta[x]$, to its offline PVar, $\widehat{\text{PVar}}_{\phi, \theta_0}[x]$, by introducing the PVar of the (unobserved) ground-truth reward r^* as an intermediate anchor. The difference between any two PVar terms can be bounded by the maximum difference between their underlying reward functions (over responses y) and the total variation distance between their sampling distributions for that x . Summing these bounds yields a relationship of the form $\text{PVar}_\theta[x] \leq \widehat{\text{PVar}}_{\phi, \theta_0}[x] + \Xi(x; \theta, \phi)$. Substituting this into the bound from Theorem 4.1 yields the final result. The full proof is in Appendix C.

Practical Implications and Discussion. Theorem 4.1 provides the core intuition: low PVar implies small gradients. Theorem 4.2 provides the formal justification for our practical data selection method. It shows that for any given prompt x , selecting it based on a high offline PVar ($\text{PVar}_{\phi, \theta_0}[x]$) is effective because this term directly contributes to a higher upper bound on its own online training gradient. This justifies why filtering for high PVar prompts leads to more impactful training updates on average.

Our approach’s effectiveness assumes the PVar signal is not dominated by error terms. The DPO objective inherently constrains policy drift through its implicit KL-divergence penalty, which, by Pinsker’s inequality, also bounds the policy distribution shift. Our strong empirical results suggest these error terms are sufficiently controlled in practice, making offline PVar an effective proxy for identifying information-rich data.

5 Experiment

We design experiments to answer two questions: (1) *Does prompt-level preference variance correlate with gradient magnitudes in actual DPO training?* (2) *Does leveraging this variance lead to improved training outcomes or model performance?* To answer these questions, we conducted three sets of experiments. First, we analyzed the training loss by dividing the DPO training prompts into three distinct subsets based on their PVar (Top 50%, Bottom 50%, and Random 50%), and comparing convergence rates and final loss values. Then, we evaluated model performance across different benchmarks (AlpacaEval 2.0 and Arena-Hard) using the same subset division strategy. Finally, to simulate real-world deployment scenarios, we train model with the top 10% of human-annotated pairs from UltraFeedback (selected by PVar) and compare with the model training with the complete human-annotated dataset, demonstrating improvements in model performance with significantly fewer training examples. More experiments and analysis can be found at Appendix D.

5.1 Setup

Models: We use the following base models for fine-tuning LLMs: Mistral-7B-Instruct-v0.2, an instruction fine-tuned version of Mistral-7B-v0.2 [Jiang et al., 2023], and Llama-3.1-8B-Instruct, an instruction finetuned version of Llama-3.1-8B [Grattafiori et al., 2024]. We use the Skywork-Reward-Llama-3.1-8B-v0.2 [Liu et al., 2024b] as the reward model to estimate the PVar except for those in Table 2. We use Llama-3.1-8B-Instruct in all of our experiments except for those in Table 1.

Training Datasets: We use a diverse mix of datasets for training, including: **UltraFeedback** [Cui et al., 2023], a large-scale dataset with 60K diverse prompts; **Chatbot Arena Conversations** [Zheng et al., 2023], containing 33K real-world user conversations; **HH-RLHF** [Bai et al., 2022], a human preference dataset from Anthropic with over 160K comparisons focused on helpfulness and harmlessness; and **WebGPT** [Nakano et al., 2021], which consists of 20K question-answer pairs for fact-intensive, web-sourced tasks.

Benchmarks: Following previous works [Meng et al., 2024, Deng et al., 2025, Wu et al., 2024, Chen et al., 2025b], we use **AlpacaEval 2.0** [Dubois et al., 2024] and **Arena-Hard** [Li et al., 2024a,b] as our evaluation benchmarks. More information for these benchmarks can be found at Appendix D.

Implementation Details: We employed the AdamW optimizer with standard parameters. Key hyperparameters for DPO training include a learning rate of 5×10^{-7} with a cosine schedule and 0.1 warmup ratio, a global batch size of 32, and a DPO β of 0.1. All models were trained for two epochs. A comprehensive list of all hyperparameters and generation settings can be found in Appendix D.

5.2 Main Results

PVar Distribution Analysis. We analyze the distribution of PVar across prompts in the left and middle panels of Figure 2. For each prompt in both datasets, we generate 5 responses and calculate the empirical PVar. The distributions from both datasets reveal similar patterns. We observe a wide range of PVar values (from near 0 to the maximum of 0.25), indicating significant variation in the strength of preference signals across prompts. Both distributions show that a substantial portion of prompts have relatively high PVar, suggesting that many examples in these datasets are informative for DPO. This consistency across different prompt collections indicates that our PVar-based analysis is robust.

Training Loss Analysis. The right panel Figure 2 illustrates the training loss curves for models fine-tuned on different subsets of data selected using PVar. We divided the training data into three distinct subsets based on their PVar: Top 50% (highest PVar), Bottom 50% (lowest PVar), and Random 50% (randomly selected examples), then separately trained models on each of these subsets. The visualization reveals distinct learning patterns. Models trained on the Top 50% subset demonstrate noticeably faster loss reduction and ultimately converge to a lower final loss value. In contrast, models trained on the Bottom 50% subset exhibit the slowest convergence rate and settle at a higher final loss.

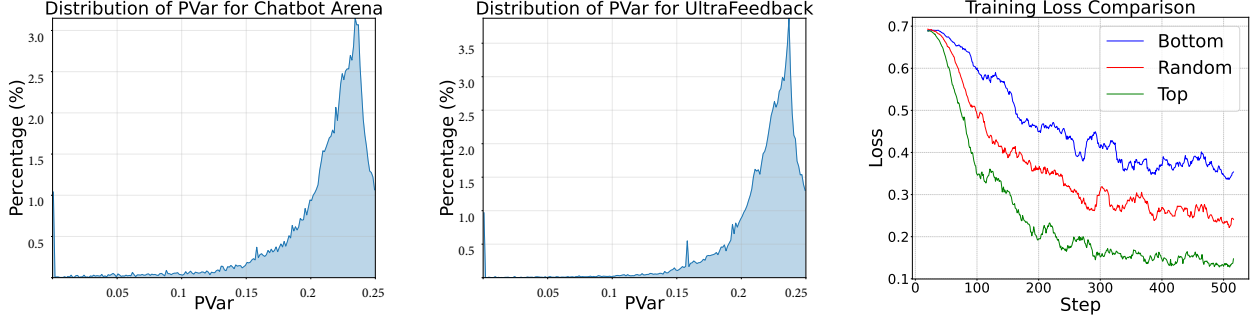


Figure 2: Left and middle: Distribution of Preference Variance (PVar) across prompts from two different datasets: Chatbot Arena Conversation and UltraFeedback. Each PVar is calculated using 5 responses generated by Llama 3.1-8B-Instruct. The distributions show a wide spread of PVar values, indicating significant variation in the informativeness of prompts, with a substantial portion exhibiting moderate-to-high PVar values. Right: Training loss curves for models fine-tuned on different data subsets selected based on PVar. The Top 50% subset (green) demonstrates faster convergence and reaches a lower final loss compared to Random 50% (red) and Bottom 50% (blue) selections, indicating more efficient learning from high-PVar training examples.

The Random 50% selection shows intermediate performance. These observations align with our theoretical analysis, providing evidence that prioritizing high-PVar examples leads to more efficient learning.

Base Model	Training Set	Selection	AlpacaEval 2.0		Arena-Hard
			LC (%)	WR (%)	WR (%)
Llama 3.1-8B-Instruct	UltraFeedback	Top	36.2	40.9	32.2
		Random	34.9	39.3	31.0
		Bottom	34.8	38.6	30.7
	Chatbot Arena	Top	36.2	39.6	30.0
		Random	33.6	39.3	28.8
		Bottom	32.9	37.5	29.2
Mistral-7B-Instruct-v0.2	UltraFeedback	Top	31.2	36.1	19.6
		Random	31.0	36.1	17.7
		Bottom	30.1	35.1	18.8
	Chatbot Arena	Top	32.5	34.5	20.4
		Random	29.1	31.6	18.0
		Bottom	28.2	30.7	16.7

Table 1: Performance comparison of different prompt selection strategies. We partition each dataset into three segments (Top 50%, Random 50%, and Bottom 50%) based on PVar. For these experiments, winning and losing responses were determined by selecting generated responses with the highest and lowest scores from our reward model. Results show that training on top-ranked prompts consistently outperforms random and bottom selection across different base models and datasets. Bold numbers indicate the best performance within each model-dataset combination.

Analysis on Different Benchmarks. Following our previous methodology, we divide the data into three subsets: Top, Random, and Bottom based on PVar, each containing 50% of the prompts, and then separately trained models on each. We use responses with the highest and lowest rewards (given by Skywork-Reward-Llama-3.1-8B-v0.2) as the chosen and rejected responses, respectively. Table 1 presents a comprehensive evaluation across different base models and training datasets. The results demonstrate a consistent trend: training with top-PVar prompts yields performance that is consistently as good as or better than random selection, and often superior, particularly on the length-controlled win rate metric. Specifically, for Llama 3.1-8B-Instruct trained on UltraFeedback, the Top 50% selection achieves a 36.2% length-controlled win rate on AlpacaEval 2.0, outperforming both random (34.9%) and bottom (34.8%) selection. This trend holds across models, datasets, and evaluation metrics, providing compelling evidence that intelligent prompt selection can enhance model performance.

PVar’s Robustness: Outperforming the Reward Gap Across Varying Reward Model Quality. We demonstrate PVar’s robustness by showing it consistently outperforms a common reward gap baseline using various size of reward models. This baseline selects the top 50% of prompts with the largest reward difference between any two responses

Dataset	Skywork-Reward Model	Selection Strategy	Win Rate (%)	LC Win Rate (%)
HH-RLHF	Llama-3.1-8B-v0.2	PVar Top	40.9	35.1
		Reward Gap Top	38.9	34.7
		PVar Bottom	38.0	35.0
	Llama-3.2-3B-v0.2	PVar Top	41.1	35.8
		Reward Gap Top	39.1	33.7
		PVar Bottom	39.0	34.9
	Llama-3.2-1B-v0.2	PVar Top	39.9	36.4
		Reward Gap Top	38.9	35.3
		PVar Bottom	38.2	33.8
WebGPT	Llama-3.1-8B-v0.2	PVar Top	40.9	35.4
		Reward Gap Top	39.5	34.9
		PVar Bottom	37.8	33.7
	Llama-3.2-3B-v0.2	PVar Top	40.6	36.3
		Reward Gap Top	38.9	34.6
		PVar Bottom	38.2	33.6
	Llama-3.2-1B-v0.2	PVar Top	40.1	35.2
		Reward Gap Top	38.6	34.3
		PVar Bottom	38.1	34.1

Table 2: Robustness of selection strategies across different reward models. We train Llama-3.1-8B-Instruct on HH-RLHF and WebGPT datasets, using three different reward models to guide prompt selection. ‘PVar Top’ consistently outperforms the ‘Reward Gap Top’ baseline, demonstrating its robustness. Bold indicates the best result within each dataset-reward model group.

Model Configuration	AlpacaEval 2.0		Arena-Hard
	LC (%)	WR (%)	WR (%)
Llama 3.1-8B-Instruct (Base Model)	24.8	24.2	21.3
+ DPO w. 10% Human Data (Final)	34.3	37.0	30.3
+ DPO w. 100% Human Data (Peak Perf. @ 64.4% Data)	32.5	36.5	29.1
+ DPO w. 100% Human Data (Final Perf.)	32.5	36.4	28.8

Table 3: Impact of selective DPO training using high-PVar prompts from UltraFeedback with human annotations. Results show that training with only the top 10% of prompts (selected via PVar) yields superior performance compared to using the full dataset, even when the full-dataset model has seen over six times more data. Bold indicates the best result.

[Deng et al., 2025, Cui et al., 2025, Khaki et al., 2024]. We evaluated both selection methods on HH-RLHF and WebGPT using three reward models of varying sizes (1B, 3B, and 8B). As detailed in Table 2, the PVar Top 50% subset yields superior performance in all configurations. The performance gap widens significantly with the less reliable 1B reward model, confirming that PVar is a more stable indicator of learning value than reward gap, particularly in the presence of noisy reward signals.

Efficient DPO with Selected Human Annotations. To simulate practical deployment scenarios, this experiment uses the UltraFeedback dataset with its original human-annotated response pairs. We first identified the top 10% of prompts with the highest PVar, then trained a model using only the human-labeled response pairs corresponding to these prompts. We compared this selective approach to training with all human-labeled pairs, evaluating the full-data model at checkpoints every 2000 steps. We trained both models for two full epochs over their respective datasets.

Table 3 shows a compelling result: training with just 10% of the data achieves a final win rate of 37.0% on AlpacaEval 2.0, which is significantly higher than the *peak performance* (36.5%) of the model trained on the full dataset. The full-data model reaches this peak after training on approximately 64.4% of the data, meaning our method achieves a better final model with over six times less data. This supports our hypothesis that focusing on high-signal, high-PVar data leads to both a more efficient process and a better final model.

6 Conclusion

In this paper, we establish a direct link between Preference Variance (PVar) and the effectiveness of DPO training. Our theoretical analysis shows, and empirical results confirm, that high-PVar prompts generate larger gradient updates, leading to faster convergence and superior model performance. Across multiple models and datasets, training on high-PVar subsets consistently outperformed using random or low-PVar data. Most notably, we found that training on only the top 10% of human-annotated high-PVar prompts surpassed training on the full dataset, demonstrating a path to significantly reduce annotation costs without sacrificing performance. This work provides a practical, theoretically grounded method for identifying high-value training data, enabling more efficient resource allocation in LLM alignment.

References

- Long Ouyang, Jeffrey Wu, Xu Jiang, Diogo Almeida, Carroll Wainwright, Pamela Mishkin, Chong Zhang, Sandhini Agarwal, Katarina Slama, Alex Ray, et al. Training language models to follow instructions with human feedback. *Advances in neural information processing systems*, 35:27730–27744, 2022a.
- Josh Achiam, Steven Adler, Sandhini Agarwal, Lama Ahmad, Ilge Akkaya, Florencia Leoni Aleman, Diogo Almeida, Janko Altschmidt, Sam Altman, Shyamal Anadkat, et al. Gpt-4 technical report. *arXiv preprint arXiv:2303.08774*, 2023.
- Minbeom Kim, Kang il Lee, Seongho Joo, Hwaran Lee, Thibaut Thonet, and Kyomin Jung. Drift: Decoding-time personalized alignments with implicit user preferences, 2025. URL <https://arxiv.org/abs/2502.14289>.
- Tianhao Shen, Renren Jin, Yufei Huang, Chuang Liu, Weilong Dong, Zishan Guo, Xinwei Wu, Yan Liu, and Deyi Xiong. Large language model alignment: A survey. *arXiv preprint arXiv:2309.15025*, 2023.
- Jiacheng Guo, Yue Wu, Jiahao Qiu, Kaixuan Huang, Xinzhe Juan, Ling Yang, and Mengdi Wang. Temporal consistency for llm reasoning process error identification. *arXiv preprint arXiv:2503.14495*, 2025.
- Miaomiao Ji, Yanqiu Wu, Zhibin Wu, Shoujin Wang, Jian Yang, Mark Dras, and Usman Naseem. A survey on progress in llm alignment from the perspective of reward design. *arXiv preprint arXiv:2505.02666*, 2025.
- Paul F Christiano, Jan Leike, Tom Brown, Miljan Martic, Shane Legg, and Dario Amodei. Deep reinforcement learning from human preferences. *Advances in neural information processing systems*, 30, 2017.
- Daniel M Ziegler, Nisan Stiennon, Jeffrey Wu, Tom B Brown, Alec Radford, Dario Amodei, Paul Christiano, and Geoffrey Irving. Fine-tuning language models from human preferences. *arXiv preprint arXiv:1909.08593*, 2019.
- Kimin Lee, Laura Smith, and Pieter Abbeel. Pebble: Feedback-efficient interactive reinforcement learning via relabeling experience and unsupervised pre-training. *arXiv preprint arXiv:2106.05091*, 2021.
- Kaixuan Huang, Yuanhao Qu, Henry Cousins, William A Johnson, Di Yin, Mihir Shah, Denny Zhou, Russ Altman, Mengdi Wang, and Le Cong. Crispr-gpt: An llm agent for automated design of gene-editing experiments. *arXiv preprint arXiv:2404.18021*, 2024.
- Kaixuan Huang, Jiacheng Guo, Zihao Li, Xiang Ji, Jiawei Ge, Wenzhe Li, Yingqing Guo, Tianle Cai, Hui Yuan, Runzhe Wang, et al. Math-perturb: Benchmarking llms’ math reasoning abilities against hard perturbations. *arXiv preprint arXiv:2502.06453*, 2025.
- John Schulman, Filip Wolski, Prafulla Dhariwal, Alec Radford, and Oleg Klimov. Proximal policy optimization algorithms, 2017. URL <https://arxiv.org/abs/1707.06347>.
- Rafael Rafailov, Archit Sharma, Eric Mitchell, Christopher D Manning, Stefano Ermon, and Chelsea Finn. Direct preference optimization: Your language model is secretly a reward model. *Advances in Neural Information Processing Systems*, 36:53728–53741, 2023.
- Ralph Allan Bradley and Milton E Terry. Rank analysis of incomplete block designs: I. the method of paired comparisons. *Biometrika*, 39(3/4):324–345, 1952.
- Yue Wu, Zhiqing Sun, Huizhuo Yuan, Kaixuan Ji, Yiming Yang, and Quanquan Gu. Self-play preference optimization for language model alignment. *arXiv preprint arXiv:2405.00675*, 2024.
- Mohammad Gheshlaghi Azar, Zhaohan Daniel Guo, Bilal Piot, Remi Munos, Mark Rowland, Michal Valko, and Daniele Calandriello. A general theoretical paradigm to understand learning from human preferences. In *International Conference on Artificial Intelligence and Statistics*, pages 4447–4455. PMLR, 2024.
- Kawin Ethayarajh, Winnie Xu, Niklas Muennighoff, Dan Jurafsky, and Douwe Kiela. Model alignment as prospect theoretic optimization. In *Forty-first International Conference on Machine Learning*, 2024.

- Hanyang Zhao, Genta Indra Winata, Anirban Das, Shi-Xiong Zhang, David D Yao, Wenpin Tang, and Sambit Sahu. Rainbowpo: A unified framework for combining improvements in preference optimization. *arXiv preprint arXiv:2410.04203*, 2024.
- Yu Meng, Mengzhou Xia, and Danqi Chen. Simpo: Simple preference optimization with a reference-free reward. *Advances in Neural Information Processing Systems*, 37:124198–124235, 2024.
- Xun Deng, Han Zhong, Rui Ai, Fuli Feng, Zheng Wang, and Xiangnan He. Less is more: Improving llm alignment via preference data selection. *arXiv preprint arXiv:2502.14560*, 2025.
- Syrine Belakaria, Joshua Kazdan, Charles Marx, Chris Cundy, Willie Neiswanger, Sanmi Koyejo, Barbara E. Engelhardt, and Stefano Ermon. Sharpe ratio-guided active learning for preference optimization in rlhf. *arXiv preprint arXiv:2503.22137*, 2025.
- Duan Yu Feng, Bowen Qin, Chen Huang, Zheng Zhang, and Wenqiang Lei. Towards analyzing and understanding the limitations of dpo: A theoretical perspective. *arXiv preprint arXiv:2404.04626*, 2024.
- Noam Razin, Zixuan Wang, Hubert Strauss, Stanley Wei, Jason D Lee, and Sanjeev Arora. What makes a reward model a good teacher? an optimization perspective. *arXiv preprint arXiv:2503.15477*, 2025.
- Ganqu Cui, Lifan Yuan, Ning Ding, Guanming Yao, Bingxiang He, Wei Zhu, Yuan Ni, Guotong Xie, Ruobing Xie, Yankai Lin, Zhiyuan Liu, and Maosong Sun. Ultrafeedback: Boosting language models with high-quality feedback. *arXiv preprint arXiv:2310.01377*, 2023.
- Lianmin Zheng, Wei-Lin Chiang, Ying Sheng, Siyuan Zhuang, Zhonghao Wu, Yonghao Zhuang, Zi Lin, Zhuohan Li, Dacheng Li, Eric P Xing, Hao Zhang, Joseph E. Gonzalez, and Ion Stoica. Judging llm-as-a-judge with mt-bench and chatbot arena, 2023.
- Yuntao Bai, Andy Jones, Kamal Ndousse, Amanda Askell, Anna Chen, Nova DasSarma, Dana Drain, Stanislaw El-Showk, Shevlon Fort, Deep Ganguli, et al. Training a helpful and harmless assistant with reinforcement learning from human feedback. *arXiv preprint arXiv:2204.05862*, 2022.
- Reiichiro Nakano, Jacob Hilton, Suchir Balaji, Jeff Wu, Long Ouyang, Christina Kim, Christopher Hesse, Shantanu Jain, Vineet Kosaraju, William Saunders, et al. Webgpt: Browser-assisted question-answering with human feedback. In *arXiv preprint arXiv:2112.09332*, 2021.
- Yann Dubois, Balázs Galambosi, Percy Liang, and Tatsunori B Hashimoto. Length-controlled alpacaEval: A simple way to debias automatic evaluators. *arXiv preprint arXiv:2404.04475*, 2024.
- Tianle Li, Wei-Lin Chiang, Evan Frick, Lisa Dunlap, Tianhao Wu, Banghua Zhu, Joseph E Gonzalez, and Ion Stoica. From crowdsourced data to high-quality benchmarks: Arena-hard and benchbuilder pipeline. *arXiv preprint arXiv:2406.11939*, 2024a.
- Tianle Li, Wei-Lin Chiang, Evan Frick, Lisa Dunlap, Banghua Zhu, Joseph E. Gonzalez, and Ion Stoica. From live data to high-quality benchmarks: The arena-hard pipeline, April 2024b.
- Huayu Chen, Guande He, Lifan Yuan, Ganqu Cui, Hang Su, and Jun Zhu. Noise contrastive alignment of language models with explicit rewards. *arXiv preprint arXiv:2402.05369*, 2024.
- Hanze Dong, Wei Xiong, Deepanshu Goyal, Yihan Zhang, Winnie Chow, Rui Pan, Shizhe Diao, Jipeng Zhang, Kashun Shum, and Tong Zhang. Raft: Reward ranked finetuning for generative foundation model alignment. *arXiv preprint arXiv:2304.06767*, 2023.
- Tianqi Liu, Zhen Qin, Junru Wu, Jiaming Shen, Misha Khalman, Rishabh Joshi, Yao Zhao, Mohammad Saleh, Simon Baumgartner, Jialu Liu, et al. Lipo: Listwise preference optimization through learning-to-rank. *arXiv preprint arXiv:2402.01878*, 2024a.
- Feifan Song, Bowen Yu, Minghao Li, Haiyang Yu, Fei Huang, Yongbin Li, and Houfeng Wang. Preference ranking optimization for human alignment. In *Proceedings of the AAAI Conference on Artificial Intelligence*, volume 38, pages 18990–18998, 2024.
- Jiwoo Hong, Noah Lee, and James Thorne. Orpo: Monolithic preference optimization without reference model. *arXiv preprint arXiv:2403.07691*, 2024.
- Caglar Gulcehre, Tom Le Paine, Srivatsan Srinivasan, Ksenia Konyushkova, Lotte Weerts, Abhishek Sharma, Aditya Siddhant, Alex Ahern, Miaosen Wang, Chenjie Gu, et al. Reinforced self-training (rest) for language modeling. *arXiv preprint arXiv:2308.08998*, 2023.
- Ziniu Li, Tian Xu, Yushun Zhang, Yang Yu, Ruoyu Sun, and Zhi-Quan Luo. Remax: A simple, effective, and efficient method for aligning large language models. *arXiv preprint arXiv:2310.10505*, 2023a.
- Han Zhong, Zikang Shan, Guhao Feng, Wei Xiong, Xinle Cheng, Li Zhao, Di He, Jiang Bian, and Liwei Wang. Dpo meets ppo: Reinforced token optimization for rlhf. *arXiv preprint arXiv:2404.18922*, 2024.

- Souradip Chakraborty, Jiahao Qiu, Hui Yuan, Alec Koppel, Furong Huang, Dinesh Manocha, Amrit Singh Bedi, and Mengdi Wang. Maxmin-rlhf: Alignment with diverse human preferences. *arXiv preprint arXiv:2402.08925*, 2024.
- Mucong Ding, Souradip Chakraborty, Vibhu Agrawal, Zora Che, Alec Koppel, Mengdi Wang, Amrit Bedi, and Furong Huang. Sail: Self-improving efficient online alignment of large language models. *arXiv preprint arXiv:2406.15567*, 2024.
- Souradip Chakraborty, Sujay Bhatt, Udari Madhushani Sehwag, Soumya Suvra Ghosal, Jiahao Qiu, Mengdi Wang, Dinesh Manocha, Furong Huang, Alec Koppel, and Sumitra Ganesh. Collab: Controlled decoding using mixture of agents for llm alignment. *arXiv preprint arXiv:2503.21720*, 2025.
- Peter Chen, Xiaopeng Li, Ziniu Li, Xi ChenD, and Tianyi Lin. Stepwise guided policy optimization: Coloring your incorrect reasoning in grpo. 2025a.
- Nirjhar Das, Souradip Chakraborty, Aldo Pacchiano, and Sayak Ray Chowdhury. Active preference optimization for sample efficient rlhf. *arXiv preprint arXiv:2402.10500*, 2024a.
- Yihan Du, Anna Winnicki, Gal Dalal, Shie Mannor, and R Srikant. Exploration-driven policy optimization in rlhf: Theoretical insights on efficient data utilization. *arXiv preprint arXiv:2402.10342*, 2024.
- Xiang Ji, Huazheng Wang, Minshuo Chen, Tuo Zhao, and Mengdi Wang. Provable benefits of policy learning from human preferences in contextual bandit problems. *arXiv preprint arXiv:2307.12975*, 2023.
- Ellen Novoseller, Yibing Wei, Yanan Sui, Yisong Yue, and Joel Burdick. Dueling posterior sampling for preference-based reinforcement learning. In *Conference on Uncertainty in Artificial Intelligence*, pages 1029–1038. PMLR, 2020.
- Aldo Pacchiano, Aadirupa Saha, and Jonathan Lee. Dueling rl: reinforcement learning with trajectory preferences. *arXiv preprint arXiv:2111.04850*, 2021.
- Yuanhao Wang, Qinghua Liu, and Chi Jin. Is rlhf more difficult than standard rl? a theoretical perspective. *Advances in Neural Information Processing Systems*, 36:76006–76032, 2023.
- Runzhe Wu and Wen Sun. Making rl with preference-based feedback efficient via randomization. *arXiv preprint arXiv:2310.14554*, 2023.
- Wei Xiong, Hanze Dong, Chenlu Ye, Ziqi Wang, Han Zhong, Heng Ji, Nan Jiang, and Tong Zhang. Iterative preference learning from human feedback: Bridging theory and practice for rlhf under kl-constraint. *arXiv preprint arXiv:2312.11456*, 2023.
- Yichong Xu, Ruosong Wang, Lin Yang, Aarti Singh, and Artur Dubrawski. Preference-based reinforcement learning with finite-time guarantees. *Advances in Neural Information Processing Systems*, 33:18784–18794, 2020.
- Zihao Li, Zhuoran Yang, and Mengdi Wang. Reinforcement learning with human feedback: Learning dynamic choices via pessimism, 2023b. URL <https://arxiv.org/abs/2305.18438>.
- Zihao Li, Xiang Ji, Minshuo Chen, and Mengdi Wang. Policy evaluation for reinforcement learning from human feedback: A sample complexity analysis. In *International Conference on Artificial Intelligence and Statistics*, pages 2737–2745. PMLR, 2024c.
- Hao Sun, Yunyi Shen, and Jean-Francois Ton. Rethinking reward modeling in preference-based large language model alignment. In *The Thirteenth International Conference on Learning Representations*, 2025.
- Noam Razin, Hattie Zhou, Omid Saremi, Vimal Thilak, Arwen Bradley, Preetum Nakkiran, Joshua Susskind, and Etai Littwin. Vanishing gradients in reinforcement finetuning of language models. *arXiv preprint arXiv:2310.20703*, 2023.
- Long Ouyang, Jeff Wu, Xu Jiang, Diogo Almeida, Clara Wainwright, Pamela Mishkin, Chong Zhang, Sandhini Agarwal, Katarina Slama, Alex Ray, John Schulman, Jacob Hilton, Fraser Kelton, Luke Miller, Maddie Simens, Amanda Askell, Peter Welinder, Paul Christiano, Jan Leike, and Ryan Lowe. Training language models to follow instructions with human feedback. In *Advances in Neural Information Processing Systems (NeurIPS)*, volume 35, pages 27730–27744, 2022b.
- Larry Wasserman. *All of statistics: a concise course in statistical inference*. Springer Science & Business Media, 2013.
- Albert Q. Jiang, Alexandre Sablayrolles, Arthur Mensch, Chris Bamford, Devendra Singh Chaplot, Diego de las Casas, Florian Bressand, Gianna Lengyel, Guillaume Lample, Lucile Saulnier, L  lio Renard Lavaud, Marie-Anne Lachaux, Pierre Stock, Teven Le Scao, Thibaut Lavril, Thomas Wang, Timoth  e Lacroix, and William El Sayed. Mistral 7b, 2023. URL <https://arxiv.org/abs/2310.06825>.
- Aaron Grattafiori, Abhimanyu Dubey, Abhinav Jauhri, Abhinav Pandey, Abhishek Kadian, Ahmad Al-Dahle, Aiesha Letman, Akhil Mathur, Alan Schelten, Alex Vaughan, et al. The llama 3 herd of models. *arXiv preprint arXiv:2407.21783*, 2024.

- Chris Yuhao Liu, Liang Zeng, Jiakai Liu, Rui Yan, Jujie He, Chaojie Wang, Shuicheng Yan, Yang Liu, and Yahui Zhou. Skywork-reward: Bag of tricks for reward modeling in llms. *arXiv preprint arXiv:2410.18451*, 2024b.
- Peter Chen, Xi Chen, Wotao Yin, and Tianyi Lin. Compo: Preference alignment via comparison oracles. *arXiv preprint arXiv:2505.05465*, 2025b.
- Guofeng Cui, Pichao Wang, Yang Liu, Zemian Ke, Zhu Liu, and Vimal Bhat. Crpo: Confidence-reward driven preference optimization for machine translation. *arXiv preprint arXiv:2501.13927*, 2025.
- Saeed Khaki, JinJin Li, Lan Ma, Liu Yang, and Prathap Ramachandra. Rs-dpo: A hybrid rejection sampling and direct preference optimization method for alignment of large language models. *arXiv preprint arXiv:2402.10038*, 2024.
- Fredrik Olsson. A literature survey of active machine learning in the context of natural language processing. 2009.
- Azar Alizadeh, Pooya Tavallali, Mohammad R Khosravi, and Mukesh Singhal. Survey on recent active learning methods for deep learning. In *Advances in Parallel & Distributed Processing, and Applications: Proceedings from PDPTA’20, CSC’20, MSV’20, and GCC’20*, pages 609–617. Springer, 2021.
- Pengzhen Ren, Yun Xiao, Xiaojun Chang, Po-Yao Huang, Zhihui Li, Brij B Gupta, Xiaojiang Chen, and Xin Wang. A survey of deep active learning. *ACM computing surveys (CSUR)*, 54(9):1–40, 2021.
- Swabha Swayamdipta, Roy Schwartz, Nicholas Lourie, Yizhong Wang, Hannaneh Hajishirzi, Noah A Smith, and Yejin Choi. Dataset cartography: Mapping and diagnosing datasets with training dynamics. *arXiv preprint arXiv:2009.10795*, 2020.
- Xun Deng, Wenjie Wang, Fuli Feng, Hanwang Zhang, Xiangnan He, and Yong Liao. Counterfactual active learning for out-of-distribution generalization. In *Proceedings of the 61st Annual Meeting of the Association for Computational Linguistics (Volume 1: Long Papers)*, pages 11362–11377, 2023.
- Nirjhar Das, Souradip Chakraborty, Aldo Pacchiano, and Sayak Ray Chowdhury. Provably sample efficient rlhf via active preference optimization. *arXiv e-prints*, pages arXiv–2402, 2024b.
- Viraj Mehta, Vikramjeet Das, Ojash Neopane, Yijia Dai, Ilija Bogunovic, Jeff Schneider, and Willie Neiswanger. Sample efficient reinforcement learning from human feedback via active exploration. *arXiv preprint arXiv:2312.00267*, 2023.
- William Muldrew, Peter Hayes, Mingtian Zhang, and David Barber. Active preference learning for large language models. *arXiv preprint arXiv:2402.08114*, 2024.
- Shenao Zhang, Donghan Yu, Hiteshi Sharma, Han Zhong, Zhihan Liu, Ziyi Yang, Shuohang Wang, Hany Hassan, and Zhaoran Wang. Self-exploring language models: Active preference elicitation for online alignment. *arXiv preprint arXiv:2405.19332*, 2024.
- Yihan Cao, Yanbin Kang, Chi Wang, and Lichao Sun. Instruction mining: Instruction data selection for tuning large language models. *arXiv preprint arXiv:2307.06290*, 2023.
- Ming Li, Yong Zhang, Shwai He, Zhitao Li, Hongyu Zhao, Jianzong Wang, Ning Cheng, and Tianyi Zhou. Superfiltering: Weak-to-strong data filtering for fast instruction-tuning. *arXiv preprint arXiv:2402.00530*, 2024d.
- Mengzhou Xia, Sathika Malladi, Suchin Gururangan, Sanjeev Arora, and Danqi Chen. Less: Selecting influential data for targeted instruction tuning. *arXiv preprint arXiv:2402.04333*, 2024.
- Yann Dubois, Chen Xuechen Li, Rohan Taori, Tianyi Zhang, Ishaan Gulrajani, Jimmy Ba, Carlos Guestrin, Percy S Liang, and Tatsunori B Hashimoto. AlpacaFarm: A simulation framework for methods that learn from human feedback. *Advances in Neural Information Processing Systems*, 36:30039–30069, 2023.

A Additional Related Work

Active Learning in LLM Fine-tuning. Active learning strategies play a crucial role in LLM fine-tuning, addressing the substantial resources required for data preparation and labeling [Olsson, 2009, Alizadeh et al., 2021]. While some work focus on selecting the most informative samples from unlabeled pools using acquisition functions based on uncertainty, diversity, or exploration principles [Ren et al., 2021], applying these techniques to RLHF and LLM fine-tuning presents unique challenges due to model scale and non-convexity. Recent work has begun addressing data selection for LLM post-training, motivated by observations that LLM training converges rapidly and excessive data can lead to performance degradation through overfitting or exposure to harmful content [Swayamdipta et al., 2020, Deng et al., 2023]. Several researchers have formulated active learning for RLHF and DPO as offline contextual dueling bandit problems [Das et al., 2024b, Mehta et al., 2023], proposing uncertainty-based approaches that measure variance in predicted logits or algorithms with theoretical guarantees on regret and query complexity. Other approaches filter prompts based on predictive entropy and reward gaps [Muldrew et al., 2024], employ bilevel optimization favoring potentially high-reward responses [Zhang et al., 2024], or use online exploration and rejection sampling strategies formulated as reverse-KL-regularized contextual bandits [Xiong et al., 2023]. In parallel work on instruction tuning, researchers have developed methods to identify high-quality subsets from large instruction datasets by adapting active learning query strategies to assess sample uncertainty and diversity [Cao et al., 2023, Li et al., 2024d, Xia et al., 2024]. Our work contributes to data efficiency in preference learning by providing clear criteria for identifying informative samples while filtering problematic ones, improving both DPO’s efficiency and performance.

B Proof of Theorem 4.1

Additional Notations. Let $f(\cdot; \theta)$ denote the neural network that produces logits. For a response y of length $|y|$, y_i is the i -th token and $y_{<i}$ are the preceding tokens. We use $\mathbf{e}_{y_i} \in \mathbb{R}^{|\mathcal{V}|}$ for the one-hot vector of token y_i from vocabulary \mathcal{V} , and $J_{f(x, y_{<i}; \theta)}$ for the Jacobian of $f(x, y_{<i}; \theta)$ with respect to θ . We assume the logits mapping is Lipschitz continuous, which implies the Jacobian norm is bounded.

Theorem B.1 (Formal version of Theorem 4.1). *For parameters $\theta \in \mathbb{R}^p$ and input $x \in \mathcal{X}$, the norm of the DPO loss gradient is upper bounded by:*

$$\|\nabla_{\theta} \mathcal{L}_{\text{DPO}}(\pi_{\theta}, \pi_{\text{ref}}; x)\| \leq C(x, \theta) \cdot P\text{Var}_{\theta}[x]^{1/3},$$

where $P\text{Var}_{\theta}[x] = \text{Var}_{y_i, y_j \sim \pi_{\theta}(\cdot|x)}[p_{\theta}(x; y_i, y_j)]$ and $C(x, \theta)$ is a constant defined as $C(x, \theta) := 8\beta|y|\gamma(x; \theta)$, with $|y|$ denoting the maximum response length L_{max} and $\gamma(x; \theta) := \max_{i, y_{<i}} \|J_{f(x, y_{<i}; \theta)}\|_2$.

Proof. The DPO loss gradient for a given prompt x can be expressed as:

$$\nabla_{\theta} \mathcal{L}_{\text{DPO}}(\pi_{\theta}, \pi_{\text{ref}}; x) = -\beta \mathbb{E}_{y_w, y_l \sim \pi_{\theta}(\cdot|x)}[(1 - p_{\theta}(x; y_w, y_l)) \cdot [\nabla_{\theta} \log \pi_{\theta}(y_w|x) - \nabla_{\theta} \log \pi_{\theta}(y_l|x)]]$$

where we used the fact that the expectation is over the model’s own distribution π_{θ} and $\sigma(-u) = 1 - \sigma(u)$.

For $c > 0$ to be determined later, we define $\mathcal{Y}_c := \{(y_w, y_l) : |p_{\theta}(x; y_w, y_l) - \frac{1}{2}| > c\}$, and a modified preference function:

$$\tilde{p}_{\theta}(x; y_w, y_l) := \begin{cases} p_{\theta}(x; y_w, y_l) & \text{if } (y_w, y_l) \notin \mathcal{Y}_c \\ \frac{1}{2} & \text{if } (y_w, y_l) \in \mathcal{Y}_c \end{cases}$$

We decompose the gradient into two terms, A and B , based on \tilde{p}_{θ} and $(p_{\theta} - \tilde{p}_{\theta})$:

$$\nabla_{\theta} \mathcal{L}_{\text{DPO}} = \underbrace{-\beta \mathbb{E}[(1 - \tilde{p}_{\theta}) \cdot \Delta \nabla \log \pi_{\theta}]}_A - \underbrace{\beta \mathbb{E}[(p_{\theta} - \tilde{p}_{\theta}) \cdot \Delta \nabla \log \pi_{\theta}]}_B$$

where $\Delta \nabla \log \pi_{\theta} = \nabla_{\theta} \log \pi_{\theta}(y_w|x) - \nabla_{\theta} \log \pi_{\theta}(y_l|x)$.

By construction, $|\tilde{p}_{\theta}(x; \cdot, \cdot) - 1/2| \leq c$, so $|1 - \tilde{p}_{\theta}|$ is also close to $1/2$. Following a detailed derivation similar to that in [Razin et al., 2023], we can bound the term A by leveraging the Lipschitz properties of the softmax function and the boundedness of $1 - \tilde{p}_{\theta}$. This yields:

$$\|A\| \leq 4\beta c|y|\gamma(x; \theta).$$

For term B , it is non-zero only on the set \mathcal{Y}_c . By Chebyshev’s inequality, the probability mass of this set is bounded by $P\text{Var}$:

$$\mathbb{P}((y_w, y_l) \in \mathcal{Y}_c|x) = \mathbb{P}\left(\left|p_{\theta} - \frac{1}{2}\right| > c\right) \leq \frac{\text{Var}[p_{\theta}]}{c^2} = \frac{P\text{Var}_{\theta}[x]}{c^2}.$$

The gradient term $\|\Delta \nabla \log \pi_\theta\|$ can be bounded by $4|y|\gamma(x; \theta)$. Since $|p_\theta - \tilde{p}_\theta| \leq 1$, we have:

$$\begin{aligned} \|B\| &\leq \beta \cdot \mathbb{E}[\mathbb{I}((y_w, y_l) \in \mathcal{Y}_c) \cdot |p_\theta - \tilde{p}_\theta| \cdot \|\Delta \nabla \log \pi_\theta\|] \\ &\leq \beta \cdot (4|y|\gamma(x; \theta)) \cdot \mathbb{P}((y_w, y_l) \in \mathcal{Y}_c | x) \\ &\leq 4\beta|y|\gamma(x; \theta) \frac{\text{PVar}_\theta[x]}{c^2}. \end{aligned}$$

Combining the bounds for A and B :

$$\|\nabla_\theta \mathcal{L}_{\text{DPO}}(\pi_\theta, \pi_{\text{ref}}; x)\| \leq 4\beta c|y|\gamma(x; \theta) + 4\beta|y|\gamma(x; \theta) \frac{\text{PVar}_\theta[x]}{c^2}.$$

This bound is minimized by choosing $c = (2 \cdot \text{PVar}_\theta[x])^{1/3}$, which yields:

$$\|\nabla_\theta \mathcal{L}_{\text{DPO}}(\pi_\theta, \pi_{\text{ref}}; x)\| \leq (4 \cdot 2^{1/3} + 4 \cdot 2^{-2/3})\beta|y|\gamma(x; \theta) \cdot \text{PVar}_\theta[x]^{1/3}.$$

Since $(4 \cdot 2^{1/3} + 4 \cdot 2^{-2/3}) \approx 7.56 < 8$, we can use a simpler constant, yielding the final bound. \square

C Proof of Theorem 4.2

We first introduce three foundational lemmas. Let $\mu_{\theta, x} := \pi_\theta(\cdot | x) \otimes \pi_\theta(\cdot | x)$.

Lemma C.1 (Variance Difference by Measure Change). *For any bounded function $U : \mathcal{Y}^2 \rightarrow [0, 1]$ and probability measures μ, ν on \mathcal{Y}^2 , we have $|\text{Var}_\mu(U) - \text{Var}_\nu(U)| \leq 6 \cdot \text{TV}(\mu, \nu)$, where TV is the total variation distance.*

Proof. $|\mathbb{E}_\mu[U^2] - \mathbb{E}_\nu[U^2]| \leq 2\text{TV}(\mu, \nu)\|U\|_\infty \leq 2\text{TV}$. Similarly, $|\mathbb{E}_\mu[U] - \mathbb{E}_\nu[U]| \leq 2\text{TV}$. Since $|(\mathbb{E}_\mu U)^2 - (\mathbb{E}_\nu U)^2| = |\mathbb{E}_\mu U - \mathbb{E}_\nu U| |\mathbb{E}_\mu U + \mathbb{E}_\nu U| \leq 2\text{TV} \cdot 2 = 4\text{TV}$. Combining gives 6TV . \square

Lemma C.2 (PVar Difference by Reward Change). *Let $p_1 = \sigma(r_1(y_i) - r_1(y_j))$ and $p_2 = \sigma(r_2(y_i) - r_2(y_j))$. If $\sup_y |r_1(x, y) - r_2(x, y)| \leq \Delta$ for a fixed x , then for a fixed measure μ , $|\text{PVar}[x; r_1, \mu] - \text{PVar}[x; r_2, \mu]| \leq 2\Delta$.*

Proof. By the mean value theorem, $|\sigma(u) - \sigma(v)| \leq \frac{1}{4}|u - v|$ since $\sup_t \sigma'(t) = 1/4$. Thus, $|p_1 - p_2| \leq \frac{1}{4}|(r_1(x, y_i) - r_2(x, y_i)) - (r_1(x, y_j) - r_2(x, y_j))| \leq \frac{1}{4}(2\Delta) = \frac{\Delta}{2}$. The rest of the proof follows the logic of Lemma C.1, with $|\mathbb{E}[p_1^2] - \mathbb{E}[p_2^2]| \leq \mathbb{E}[|p_1 - p_2||p_1 + p_2]| \leq 2\mathbb{E}[|p_1 - p_2|] \leq \Delta$, and $|(\mathbb{E}p_1)^2 - (\mathbb{E}p_2)^2| \leq \Delta$. Summing them yields 2Δ . \square

Lemma C.3 (TV distance of Product Measures). *For a fixed prompt x , $\text{TV}(\pi_1(\cdot | x) \otimes \pi_1(\cdot | x), \pi_2(\cdot | x) \otimes \pi_2(\cdot | x)) \leq 2 \cdot \text{TV}(\pi_1(\cdot | x), \pi_2(\cdot | x))$.*

Proof. Let $\mu_i = \pi_i(\cdot | x) \otimes \pi_i(\cdot | x)$. The TV distance is $\frac{1}{2} \int |d\mu_1 - d\mu_2|$.

$$\begin{aligned} \text{TV}(\mu_1, \mu_2) &= \frac{1}{2} \iint |\pi_1(y_1 | x) \pi_1(y_2 | x) - \pi_2(y_1 | x) \pi_2(y_2 | x)| dy_1 dy_2 \\ &= \frac{1}{2} \iint |\pi_1(y_1 | x) \pi_1(y_2 | x) - \pi_1(y_1 | x) \pi_2(y_2 | x) + \pi_1(y_1 | x) \pi_2(y_2 | x) - \pi_2(y_1 | x) \pi_2(y_2 | x)| dy_1 dy_2 \\ &\leq \frac{1}{2} \iint |\pi_1(y_1 | x) (\pi_1(y_2 | x) - \pi_2(y_2 | x))| dy_1 dy_2 + \frac{1}{2} \iint |\pi_2(y_2 | x) (\pi_1(y_1 | x) - \pi_2(y_1 | x))| dy_1 dy_2 \\ &= \frac{1}{2} \int \pi_1(y_1 | x) dy_1 \int |\pi_1(y_2 | x) - \pi_2(y_2 | x)| dy_2 + \frac{1}{2} \int \pi_2(y_2 | x) dy_2 \int |\pi_1(y_1 | x) - \pi_2(y_1 | x)| dy_1 \\ &= \text{TV}(\pi_1(\cdot | x), \pi_2(\cdot | x)) + \text{TV}(\pi_1(\cdot | x), \pi_2(\cdot | x)) = 2 \cdot \text{TV}(\pi_1(\cdot | x), \pi_2(\cdot | x)). \end{aligned}$$

\square

Proof of Theorem 4.2. Let $e_\theta(y) = \hat{r}_\theta(x, y)$. For a fixed prompt x , we use the (unobserved) ground-truth reward $r^*(x, y)$ as an anchor and apply a triangle inequality:

$$\begin{aligned} |\text{PVar}_\theta[x] - \widehat{\text{PVar}}_{\phi, \theta_0}[x]| &= |\text{PVar}[x; e_\theta, \mu_{\theta, x}] - \text{PVar}[x; r_\phi, \mu_{\theta_0, x}]| \\ &\leq |\text{PVar}[x; e_\theta, \mu_{\theta, x}] - \text{PVar}[x; r^*, \mu_{\theta, x}]| && \text{(Term 1)} \\ &\quad + |\text{PVar}[x; r^*, \mu_{\theta, x}] - \text{PVar}[x; r^*, \mu_{\theta_0, x}]| && \text{(Term 2)} \\ &\quad + |\text{PVar}[x; r^*, \mu_{\theta_0, x}] - \text{PVar}[x; r_\phi, \mu_{\theta_0, x}]| && \text{(Term 3)} \end{aligned}$$

We bound each term for the specific x :

- **Term 1 (Reward change from r^* to e_θ):** By Lemma C.2, this is bounded by $2 \sup_y |e_\theta(x, y) - r^*(x, y)|$.
- **Term 2 (Measure change from $\mu_{\theta_0, x}$ to $\mu_{\theta, x}$):** By Lemma C.1, this is bounded by $6 \cdot \text{TV}(\mu_{\theta, x}, \mu_{\theta_0, x})$.
- **Term 3 (Reward change from r_ϕ to r^*):** By Lemma C.2, this is bounded by $2 \sup_y |r_\phi(x, y) - r^*(x, y)|$.

Summing these bounds, we get:

$$\text{PVar}_\theta[x] \leq \widehat{\text{PVar}}_{\phi, \theta_0}[x] + 2 \sup_y |e_\theta(x, y) - r^*(x, y)| + 6 \text{TV}(\mu_{\theta, x}, \mu_{\theta_0, x}) + 2 \sup_y |r_\phi(x, y) - r^*(x, y)|.$$

The term $\sup_y |e_\theta(x, y) - r^*(x, y)|$ can be further bounded by $\sup_y |e_\theta(x, y) - r_\phi(x, y)| + \sup_y |r_\phi(x, y) - r^*(x, y)|$ using triangle inequality. This leads to the prompt-specific error term $\Xi(x; \theta, \phi)$ defined in the theorem statement. Now, substitute this into the result of Theorem 4.1:

$$\|\nabla_\theta \mathcal{L}_{\text{DPO}}(\pi_\theta, \pi_{\text{ref}}; x)\| \leq C(x, \theta) \cdot \left(\widehat{\text{PVar}}_{\phi, \theta_0}[x] + \Xi(x; \theta, \phi) \right)^{1/3}.$$

This concludes the proof, as the bound holds for the specific prompt x . \square

D Additional Experimental Results

Training Configuration. All experiments were conducted on 4 NVIDIA H100 GPUs. For DPO training, we used the following settings: a per-device batch size of 2 with 4 gradient accumulation steps (total global batch size of 32), a maximum prompt length of 4096, and 2 training epochs. We note that for all evaluation metrics, the standard error typically ranges between 1% and 2%.

More Information about AlpacaEval 2.0 and Arena-Hard. AlpacaEval 2.0 comprises 805 diverse prompts from AlpacaFarm [Dubois et al., 2023], covering general human instructions across various scenarios. It employs GPT-4-Turbo as a proxy for human judgment. Performance is primarily measured through win rates (WR) against the reference responses, with length-controlled win rates (LC) specifically designed to mitigate bias toward lengthy responses and encourage concise, effective answers. Arena-Hard consists of particularly difficult prompts that require advanced reasoning, knowledge application, and instruction following. Models are compared against GPT-4-0314 as the baseline. Performance is measured through win rates (WR) as determined by the GPT-4-Turbo judge.

PVar Estimation Generation. To estimate PVar for each prompt, we generated 5 responses using a maximum length of 2048, a temperature of 0.7, and top-p sampling with $p=1$.

Evaluation Generation. For evaluations on AlpacaEval 2.0 and Arena-Hard, we used a temperature of 0.7 and top-p sampling with $p=1$. We adhered to the standard maximum length settings for each benchmark: 2048 for AlpacaEval 2.0 and 4096 for Arena-Hard.

Specifics for Figures. The models used in both Figure 3 and the right panel of Figure 2 are Llama-3.1-8B Instruct, and the training dataset employed for both analyses is the Chatbot Arena Conversation dataset.

Training Margin Analysis. Figure 3 presents the training margin evolution for models fine-tuned on different subsets of data selected using PVar. The margin, calculated as the difference in model confidence scores between preferred and rejected responses, serves as an indicator of how well the model learns to distinguish between response qualities. The results reveal that models trained on the Top 50% subset (highest PVar) exhibit the most rapid margin increase during the early training phases and ultimately achieve the highest final margin values. Conversely, models trained on the Bottom 50% subset show the slowest margin growth and converge to lower final margins. The Random 50% selection demonstrates performance that falls between these two extremes. These margin dynamics support our theory that high-PVar examples provide clearer preference signals, enabling models to develop more robust preference understanding.

Ablation Study on Hyperparameter. To validate the robustness of our findings, we conduct an ablation study by varying the beta parameter to $\beta = 0.01$ in DPO training following [Deng et al., 2025]. Table 4 presents the results of this ablation experiment, maintaining the same experimental setup where data is divided into Top, Random, and Bottom subsets based on PVar. The results demonstrate that even with a different beta value, the Top selection strategy consistently outperforms Random and Bottom selections across all model-dataset combinations. This consistency across different beta values reinforces that the benefits of prioritizing high-PVar prompts in the DPO training process.

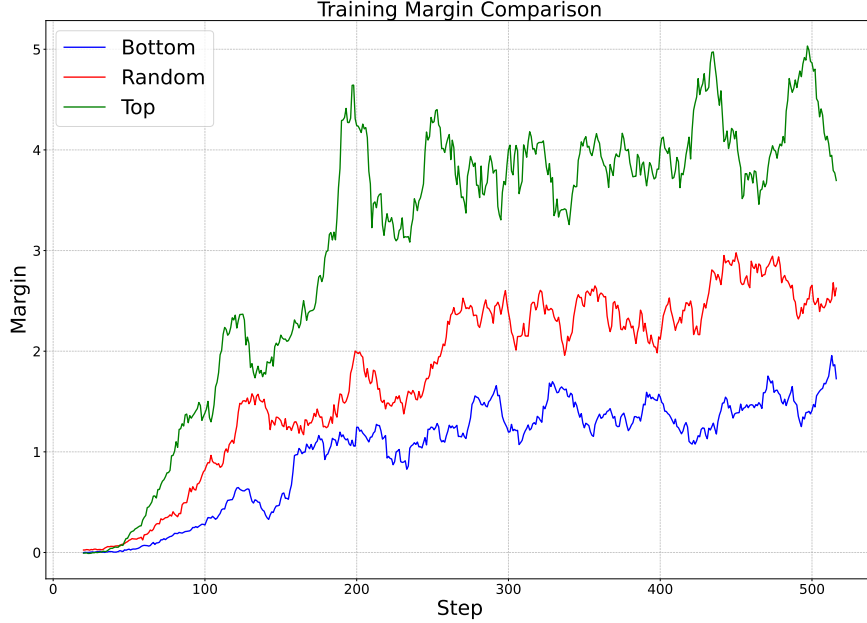


Figure 3: Training margin curves for models fine-tuned on different data subsets selected based on PVar. The margin represents the difference in model confidence between preferred and rejected responses during training. Models trained on the Top 50% subset (green) show the fastest margin increase and achieve the highest final margin values, while the Bottom 50% subset (blue) exhibits slower margin growth and lower final margins. The Random 50% selection (red) demonstrates intermediate performance, confirming that high-PVar examples facilitate more effective preference learning.

Table 4: Ablation study on beta parameter ($\beta = 0.01$) for different prompt selection strategies. Training on top-PVar prompts consistently achieves the best performance across different models and datasets. Bold numbers indicate the best performance within each model-dataset combination.

Base Model	Training Set	Selection	AlpacaEval 2.0		Arena-Hard
			LC (%)	WR (%)	WR (%)
Llama 3.1-8B-Instruct	UltraFeedback	Top	36.8	40.8	33.3
		Random	34.0	38.4	29.4
		Bottom	34.9	38.4	28.6
	Chatbot Arena	Top	36.1	39.5	32.4
		Random	35.2	39.4	30.6
		Bottom	35.0	38.6	29.4
Mistral-7B-Instruct-v0.2	UltraFeedback	Top	30.1	37.9	20.9
		Random	29.0	35.4	18.9
		Bottom	29.0	36.8	18.9
	Chatbot Arena	Top	31.3	34.4	20.4
		Random	29.8	34.3	18.0
		Bottom	30.3	34.4	16.7

E Qualitative Analysis

As qualitative examples truly illuminate the practical impact of our method. We compared models trained on Top vs. Bottom PVar data and observed clear behavioral differences.

Training on high-PVar prompts leads to a model that is more **nuanced and capable** in several key areas:

1. **Critical Thinking & Fact-Checking:** When asked "Do you know why turkeys become the official food of thanksgiving?", the **Low-PVar** model gives a lengthy explanation accepting the false premise. In contrast, the **High-PVar** model **immediately corrects the misconception**, stating, "A common myth has been debunked! Turkeys are not actually the official food of Thanksgiving..." before providing a more critical analysis.
2. **Information Organization:** For knowledge queries, the **Low-PVar** model often produces long, unstructured lists. The **High-PVar** model **organizes information with clear categorical headings** (e.g., **Jazz and Blues**, **Swing and Dance Music**), making the response more reader-friendly and logical.

These examples suggest that high-PVar prompts, which often reflect human disagreement on complex criteria, train the model to better handle the more sophisticated and nuanced aspects of language and reasoning.